Low Frequency Instability in Hybrid Rocket Combustion

Changjin Lee, Yungwhan Byun
Department of Aerospace Engineering, Konkuk University, Seoul 143-701, Korea
Email: cjlee@konkuk.ac.kr

Abstract: Hybrid rocket combustion frequently displays a sudden amplification of combustion pressures leading into low frequency instability (LFI) with peak frequency of 10~20Hz. A series of experimental tests was designed to examine the triggering mechanism of LFI. To this end, a couple of parameters was selected and the sensitivity of each parameter to instability was evaluated including volume ratios between main and post chambers, oxidizer mass flow rates, and solid fuel types. The results showed that the initiation of LFI was related with the flow modifications caused by vortex shedding and volume ratios between main and post chambers. Additional analysis was done to understand the critical role of vortex shedding on the initiation of LFI in the post chamber. Also, the CH* luminosity images and POD (Proper Orthogonal Decomposition) analysis show the lumped flow structures with time-varying intensity in unstable combustion. A periodic change in the local heat release appears to generate large-scale flow rotations, and the large-scale flow rotations are likely to be associated with the periodic flame extinction at the frequency of about 20 Hz. Also, the flame extinction seems to take a crucial role in the occurrence of LFI.
Key Words:

1. Introduction

Combustion in hybrid rocket motors is relatively a complex procedure to understand in nature because of complicated coupling with fuel regressions, convective heat transfer, and diffusional flame in the turbulent boundary layer. Hybrid rocket combustion shows usually stable characteristics compared to that of other conventional chemical rockets such as solid and liquid rockets. Nonetheless, typical pressure oscillations with a peak frequency much lower than acoustic modes were frequently observed. Even though the causes of the instability are not clearly understood yet, it is suspected that a coupling of various types of pressure oscillation is the primary cause of low frequency instability (LFI).

A summary of physical explanation of LFI mechanism in hybrid rocket motors was addressed in reference[1)]. This includes the response of low impedance oxidizer feeding system, combustion response to externally imposed pressure oscillations, periodic accumulation and break-off of melted layers from the fuel surface, and the time lag of vaporization and the combustion of liquid droplets. Each mechanism seemed to be responsible for generating a typical frequency range of oscillation based on the characteristics of primary responses. For example, low frequency oscillations (≤ 100Hz) are the results of coupling of oxidizer feeding system with pressure oscillations due to time lag responses of solid fuel. However, the unbounded high frequency pressure oscillations (>1000Hz) usually observed in solid and liquid propulsion systems were seldom found in hybrid rocket combustion. Instead, low frequency oscillations less than 50Hz were dominantly observed.

Many studies have been investigated on the initiation mechanisms of LFI. Jenkins et al.[1)] studied low frequency oscillations with a peak frequency of about 10Hz using 1-D theoretical model. In particular, they investigated a filling time of oxidizer flux in the motor as the primary causes of low frequency oscillations by using a modified characteristic length (L*). Lee[2)] theoretically suggested that a transient behavior of thermal response of the solid fuel to quasi-steady heat input from the gas phase could be the initiation mechanism of low frequency oscillations. This is generally known as thermal lag oscillations, mainly observed in solid rocket motors due to the different thermal response of gas and solid phases to heat transfer from gas phase.

Karabeyoglu et al.[3)] revealed that LFI was the results of complicated coupling of thermal lag of solid fuel with the boundary layer adjustment to external perturbations in hybrid rocket combustion. They proposed a linearized theory based on the mathematical perturbation method in order to predict the initiation of low frequency pressure oscillations. The results showed a good agreement with experimental data of pressure oscillations with a peak frequency up to 50Hz.

Boardman et al.[4)] observed sudden amplification of pressure oscillations during combustion processes. FFT analysis confirmed that the instability frequency lies in the range of less than 500Hz. A peak frequency less than 50 Hz was dominantly identified in the spectral data. But, their study did not address the causes of combustion instability of low frequency. Korting et al.[5)] also found that pressure oscillations were suddenly amplified during the combustion. Though the results did not include the spectral analysis of pressure oscillations, they suspected that the sudden increase in the regression rate was directly associated with the abrupt amplification of low frequency pressure oscillations.

Carmicino et al. [6)] performed a series of combustion tests with various injector configurations. The test results with radial type injectors showed combustion instability with a peak frequency of 10~30Hz. They suspected the resonance of pressure perturbations due to unsteady heat releases in the post chamber and acoustic excitations of the main combustor as a triggering mechanism of combustion instability. They claimed that unsteady heat release was possibly related with periodic formation of large-scale vortex shedding into the post chamber producing additional pressure perturbations. However, their study did not account for the effect of flow modifications in the different chamber configurations such as chamber volume ratio, post chamber length, fuel port diameter and etc.

Event though previous studies suggested the geometric chamber configuration could be a controlling parameter in determining the occurrence of LFI, no comprehensive study has been done to bridge the gap between experimental observations and understanding on the triggering mechanisms of LFI. In this study, a series of experimental tests was designed to investigate the triggering mechanism of LFI, which was suddenly amplified at a certain moment of the combustion. To this end, a couple of controlling parameters was selected and the sensitivity of each parameter to instability was evaluated, including volume ratios of main and post chambers, oxidizer mass flow rates, and solid fuel types. Also this study will focus on the modification in flow dynamic behaviors over the backward facing step in the post chamber by locating diaphragms at the rear end of fuel. In addition, the effect of time variation of fuel diameters on the initiation of instability was investigated.

2. Combustion tests

Fig. 2.1 shows the schematic of the experimental-setup. A series of hybrid rocket combustion tests was conducted with a lab scale motor of GOx and PMMA combinations as an oxidizer and solid fuel, respectively. An axial type injector was used in all tests. Solenoid and check valves were used to control oxidizer feeding. The maximum capacity of mass flow controller was up to 40g/sec in the tests. Nitrogen gas was used to purge after the combustion by the PLC (Programmable Logic Controller) control. Piezo-type sensors were installed to measure the combustion pressure. DAQ board and Labview program were also implemented for data acquisition process. Dimensions of the baseline fuel have 50mm and 20mm of outer and inner diameters, respectively. In the baseline configuration, the chamber length of main, pre and post chambers were fixed as 200mm, 45mm and 75mm, respectively. A water-cooled nozzle was used, in which a throat diameter and nozzle length were 6.5mm and 40mm, respectively.

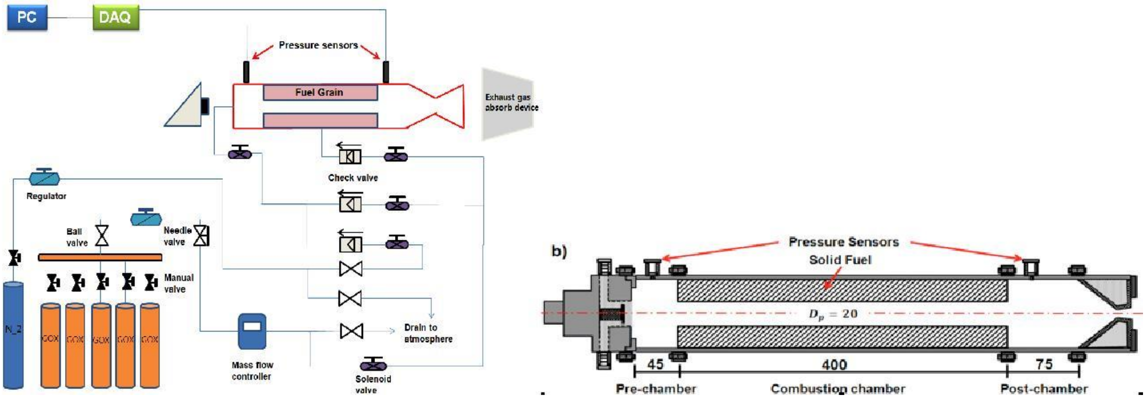

Fig. 2.1. Schematic of Test Set-up and Test 3 Configuration

Table 2.1 reports a summary of results of all test cases. A baseline test was made as a reference case, in which combustion pressure showed stable behavior and no distinctive LFI was found. Each test case has different configurations of main and post chamber length, whereas pre chamber length was kept unchanged. Here VR is the volume ratio between main and post chambers. The mass flow controller was used to control oxidizer mass flow from 10g/sec to 25g/sec for providing various O/F conditions.

The average O/F ratio was calculated by dividing total oxidizer mass by regressed fuel mass during the test. (O/F = $\int \dot{m}_{ox} dt/\Delta m_f$)

Table 2.1. Summary of combustion test results

***Nozzle throat diameter: 5.5mm**

<table>
<tr><th>Test No.</th><th>Solid Fuel</th><th>Chamber Length (mm)</th><th>Post chamber Length (mm)</th><th>Oxidizer mass flow rate (g/s)</th><th>O/F Ratio</th><th>LFI</th><th colspan="2">Remarks</th></tr>
<tr><td>Baseline</td><td>PMMA</td><td>200</td><td>75</td><td>20</td><td>5.20</td><td>No</td><td colspan="2">Reference</td></tr>
<tr><td>1</td><td>PMMA</td><td>200</td><td>105</td><td>20</td><td>5.57</td><td>No</td><td colspan="2" rowspan="5">Volume ratio between main and post chamber</td></tr>
<tr><td>2</td><td>PMMA</td><td>200</td><td>200</td><td>20</td><td>5.59</td><td>No</td></tr>
<tr><td>3</td><td>PMMA</td><td>400</td><td>75</td><td>20</td><td>2.35</td><td>Yes</td></tr>
<tr><td>4</td><td>PMMA</td><td>400</td><td>105</td><td>20</td><td>2.41</td><td>No</td></tr>
<tr><td>5</td><td>PMMA</td><td>400</td><td>200</td><td>20</td><td>2.46</td><td>No</td></tr>
<tr><td>6</td><td>PMMA</td><td>400</td><td>75</td><td>10</td><td>2.23</td><td>Yes</td><td colspan="2" rowspan="3">Oxidizer mass flow rate</td></tr>
<tr><td>7</td><td>PMMA</td><td>400</td><td>75</td><td>15</td><td>2.29</td><td>Yes</td></tr>
<tr><td>8</td><td>PMMA</td><td>400</td><td>75</td><td>25</td><td>2.43</td><td>Yes</td></tr>
<tr><td>9</td><td>PMMA</td><td>400</td><td>75</td><td>20</td><td>2.31</td><td>Yes</td><td rowspan="2">Rear diaphragm</td><td rowspan="4">Vortex shedding over a backward</td></tr>
<tr><td>10</td><td>PMMA</td><td>400</td><td>75</td><td>20</td><td>2.28</td><td>Yes</td></tr>
<tr><td>11</td><td>PMMA</td><td>400</td><td>75</td><td>20</td><td>2.23</td><td>Yes</td><td rowspan="2">Cutting rear edge</td></tr>
<tr><td>12</td><td>PMMA</td><td>400</td><td>75</td><td>20</td><td>2.32</td><td>Yes</td></tr>
<tr><td>13*</td><td>PMMA</td><td>400</td><td>75</td><td>20</td><td>2.43</td><td>Yes</td><td colspan="2">Pressure sensitive combustion regime</td></tr>
<tr><td>14</td><td>HTPB</td><td>200</td><td>75</td><td>20</td><td>3.78</td><td>No</td><td colspan="2" rowspan="2">Fuel type</td></tr>
<tr><td>15</td><td>HTPB</td><td>200</td><td>40</td><td>20</td><td>3.60</td><td>Yes</td></tr>
</table>

Tests 1 and 2 were designed to investigate the effect of post chamber length on the initiation of LFI. Test 3 was the case where the main chamber length increased as twice as that of baseline. Tests 4 and 5 were designed to examine the effect of post chamber length in Test 3. Tests 6-8 were designed to investigate the effect of variation of oxidizer mass flow rate on the amplification of pressure oscillations. Tests 9-12 were performed to examine how the formation of vortex shedding over backward facing steps can affect the initiation of LFI. Test 13 was done with a reduced throat diameter from 6.5mm of baseline case to 5.5mm to increase a chamber pressure level. The fuel regression rate is mainly governed by diffusional heat flux in the turbulent boundary layer. However, with reduced combustion pressure, the regression rate becomes pressure sensitive. In this regard, Test 13 was designed to investigate the effect of combustion pressure on the onset of instability. Finally, Tests 14-15 was carried out to investigate the responses in combustion pressure with a different solid fuel of HTPB.. The results showed that the test cases only with a volume ratio of 0.80~0.85 (Test cases 3 and 15) showed LFI. Further studies will be necessary to understand physical relations between volume ratio and the initiation of LFI.

Visualization images captured at high sampling rate are exported as a movie file. Specific frame cannot be accessed in a movie file, hence the file is decompressed to frame by frame. Original images are consisted of 3 channels representing red, green, and blue color. Each pixel contains 28 bits information in each channel and this is converted to brightness (Y) and color variance (U, V) information as shown in Fig. 2.2 The converted brightness information is used throughout the analysis. Total amount of luminosity from each image can be calculated by evaluating brightness data Y in the computer in-house software. Fig. 2.2b shows an example of captured screen evaluating luminosity data from brightness Y. The extracted brightness information represents the luminosity. Luminosity for a specific time is computed by summing all the brightness data from each pixel within the analysis domain of a frame.

Fig. 2.2. a) Extraction of brightness and luminosity estimation from captured image
b) Screen capture of image processing software

3. Combustion Pressure and spectral analysis in test 3

Test 3 was done to investigate the effect of changes in the combustion chamber volume on the initiation of LFI by increasing the main chamber length from 200mm to 400mm while the post chamber length was kept unchanged at 75mm. Note that VR in this case was 0.85. Fig. 3.1 shows the trajectory of combustion pressure in Test 3. The magnitude of peak-to-peak amplitudes suddenly increased from stable level up to around 30 psi (2.07 bar) at the moment of 14 second of combustion and lasted about three seconds. Spectral analysis showed that pressure oscillations with a peak frequency of 17Hz were dominantly appeared in the amplifications. After the end of first amplification, the second amplification with 14Hz appeared in a row at the time of 23 second as well. The amplitudes of the second amplification were less than those measured at the first one. In literature, combustion instability was defined as a case where the amplitude of pressure oscillations exceeds 5% of an average pressure. According to this criterion, oscillations in test 3 with amplitudes larger than 23% and 15% of mean pressure can be classified as the exhibition of LFI.
Note that the oxidizer flow rate in Test 3 was maintained at 20g/sec. However, pressure measurements

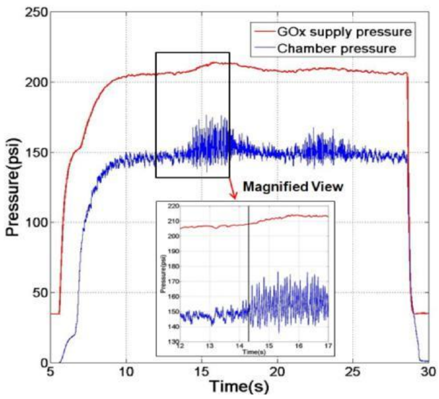

Fig. 3.1. Trajectory of combustion pressure and oxidizer supply pressure in Test 3

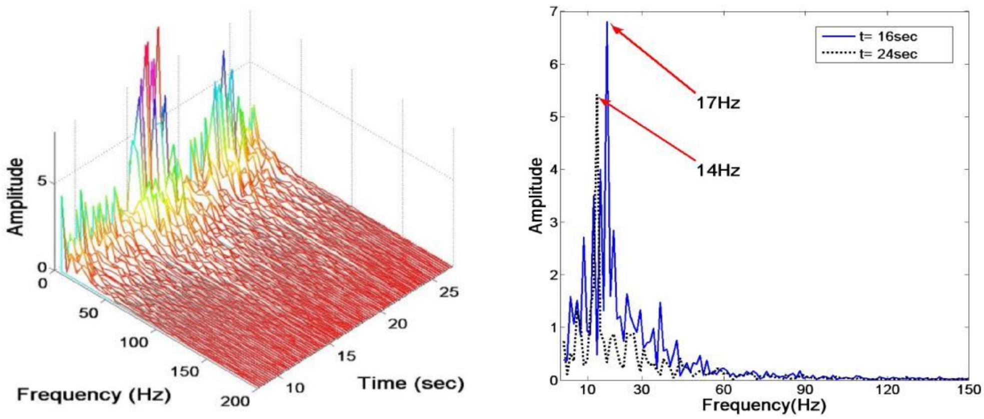

Fig. 3.2. Frequency waterfall and peak frequency of oscillation in Test 3

showed that the oxidizer supply pressure slightly increased from the mean pressure of 210 psi (14.48 bar) at the moment of LFI, because the onset of combustion instability affected to increase the supply pressure in the upstream of injectors through the flow controller. A magnified view of pressure curve in Fig. 3.1 clearly showed that the first amplification was independent of an increase in the oxidizer supply pressure.

Fig. 3.2 shows the frequency waterfall of combustion pressures in Test 3. Pressure oscillations suddenly amplified up to three times larger magnitudes than those in the baseline case. In this case, even though the peak frequency of instability was shifted toward a higher one of 14~17Hz compared to the baseline, LFI in Test 3 seems to be the result of resonating two different oscillations: pressure oscillations already existed in the baseline test and the another oscillations whose source is not clearly known yet. In this regard, Karabeyoglu et al. claimed that LFI is the result of complex coupling of thermal transients in solid fuels, known as thermal lags, and the transitional adjustment of the turbulent boundary layer to external perturbations[3)].

In general, a thermal lag in the solid fuel is known as the source of typical oscillations with a frequency of 10~30Hz determined by a solid fuel type and combustion conditions. Thus, the current study focuses on understanding the sudden amplification of pressure oscillations using the resonance of thermal lag and the unknown source of pressure perturbations. In addition, oxidizer flow rates and fuel types were also selected as control parameters to assess their sensitivity to LFI initiation.

3.1 Controlling oxidizer mass flow rate and HTPB fuel

In the tests 6-8, the oxidizer flow rate was controlled to provide different O/F conditions while other parameters were kept unchanged as used in Test 3.. Test time was set to 22 seconds for all test cases.

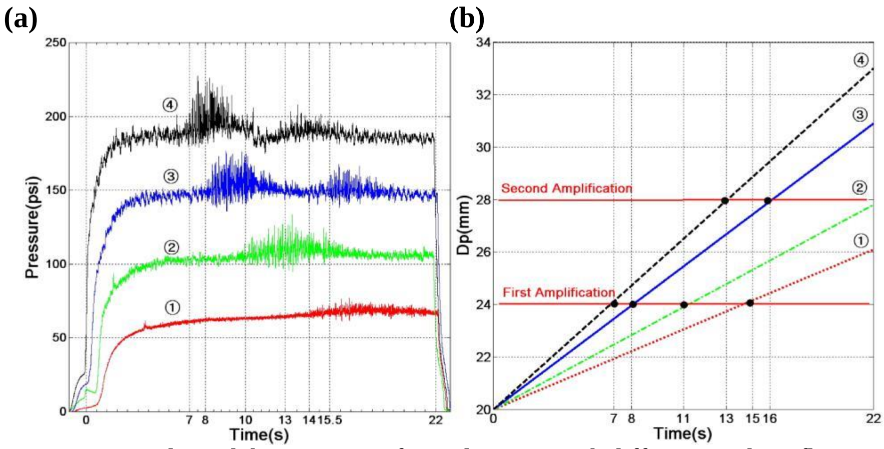

Fig. 3.1.1. P-t results and the variation of port diameter with different oxidizer flow rate ① Test 6 ② Test 7 ③ Test 3 ④ Test 8

Fig. 3.1.1 shows a summary of pressure curves with different oxidizer mass flow rates and the variation of O/F ratio in Tests 3, 6, 7 and 8 by increasing the oxidizer flow from 10g/sec to 25g/sec in each test. The pressure oscillations were amplified in all cases at a certain moment of combustion. The first amplifications happened at 7, 8, 10 and 14 seconds of combustion depending on oxidizer flow rates in each test. As seen in Fig. 5 (a), the amplification appeared at an earlier time of combustion as the oxidizer flow rate increased. However, the second amplification of oscillations was not observed in Tests 6 and 7. Also, the variation of fuel diameters during combustion is displayed in Fig. 3.1.1. (b) with two horizontal lines representing the fuel diameters at which pressure amplifications occurred respectively. Note that the regression rate in Test 3 was measured as approximately 0.25 mm/sec, which showed a good agreement with the prediction of 0.27mm/sec. The time variations of fuel diameter in Tests 3 and 6-8 were displayed altogether in Fig. 3.1.1 (b) based on the predictions of fuel regression rates in reference 7. Critical fuel diameters corresponding to pressure amplification in each test were calculated by the time variation of fuel diameters in Fig. 3.1.1 (b). And the calculation confirmed that the critical fuel diameters in Tests 6-8 were found approximately 24 and 28mm respectively. Note that the final fuel diameter in Tests 6 and 7 did not reach to a critical diameter at which the second amplification occurred. This can explain the reason why the second oscillation was not observed in

Tests 6 and 7. Even though the detailed mechanism of consecutive appearance of instability was not fully understood yet, the results showed that the initiation of LFI was not directly associated with the variation of oxidizer mass flow rates but with the variation of fuel diameters.

Tests 14-15 were carried out with different solid fuels by substituting PMMA with HTPB to explore the effect of solid fuels on the initiation of instability. Fig. 3.1.2 shows a combustion pressure trajectory in Test 15 with HTPB. The pressure oscillations were amplified immediately after the ignition developing into LFI more quickly than Test 3 with PMMA. The lower density and easy evaporating properties of HTPB are responsible for the earlier appearance of LFI than in PMMA. Generally, HTPB regressed very quickly than PMMA approaching its critical diameter where instability can be initiated.

Fig. 3.1.3 exhibits a frequency waterfall and peak frequency of combustion pressure oscillations in Test 15. The peak frequency in Test 15 was slightly shifted to higher one of about 20~30Hz than those in Test 3 with PMMA. Note that the dominant frequency of oscillations in stable combustion was mainly determined by the thermal property of solid fuel HTPB due to thermal lags. The estimation of peak frequency of HTPB combustion was found about 15~25Hz[2,3]. Thus, the occurrence of LFI in Test 15 can be the result of resonating thermal lag oscillations of HTPB with the unknown source of pressure perturbations. Therefore, the results in Tests 3, 6-8 and 15 suggest that the occurrence of LFI would be independent of either the material property, fuel composition or oxidizer mass flow. The initiation of instability seemed to be closely associated with flow modifications induced by the change in chamber configuration including main and post chamber volume and length.

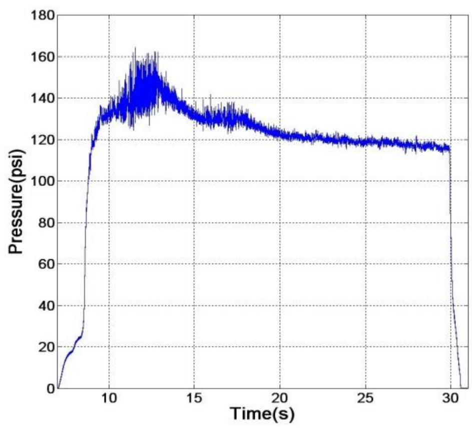

Fig. 3.1.2. Trajectory of combustion pressure in Test 15 with HTPB

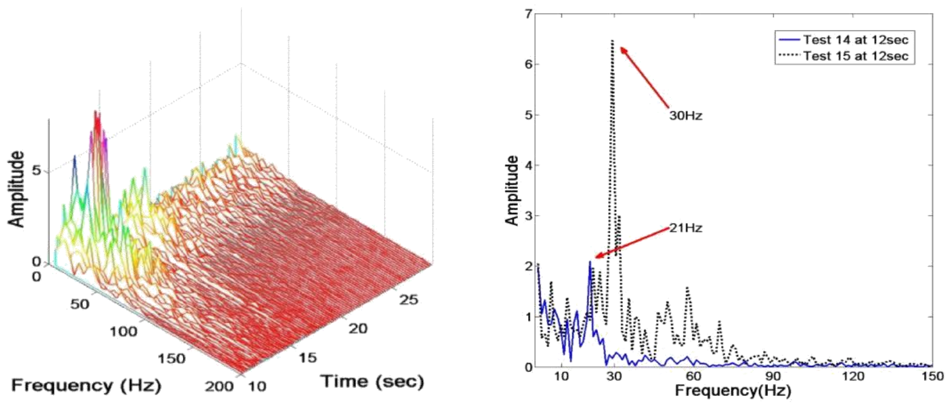

Fig. 3.1.3. FFT waterfall and peak frequency in Test 15

3.2 Fuel regression vs. The LFI occurrence

Test 8 was repeatedly done to measure the critical fuel diameter by stopping oxidizer supply at which LFI initiated. Fig. 3.2.1 shows the entire pressure curve recorded in Test 8 and a part of pressure curve terminated at the instant of LFI. Critical diameters corresponding to the first and second amplification in Test 8 were averaged with several measurements and found about 24 and 28 mm, respectively. As mentioned in the previous section, the critical diameter corresponding to the first amplification in Tests of 3, 6 and 7 was also calculated about 24 mm. This suggests that the time variation of fuel diameter takes a very important role in determining the occurrence of LFI. Since the difference in diameter between fuel grain and post chamber is step height, the time variation of fuel diameters brought into a continuous reduction in step height and consequently weakened vortex strength in the post chamber. If the initiation of LFI would be associated with the formation of vortex flow in the post chamber, the installation of diaphragm with a diameter of 24mm could artificially produce pressure perturbations, which leading to LFI during the combustion. This is one of the possible scenarios that could explain the initiation of LFI in the combustion.

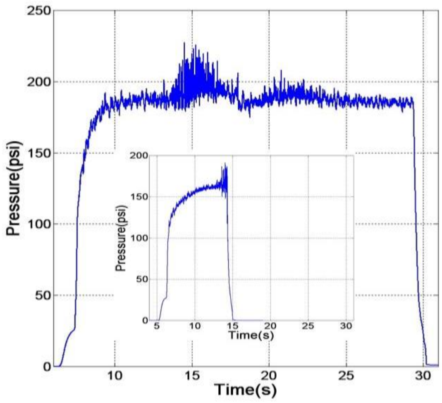

Fig. 3.2.1. Trajectory of combustion pressure in Test 8

In order to assess the sensitivity of the time variation of fuel diameters to the initiation of LFI, Tests 9 and 10 were done with different rear diaphragms. Each diaphragm has the same inner diameters of 24 and 28mm as measured in Test 8.

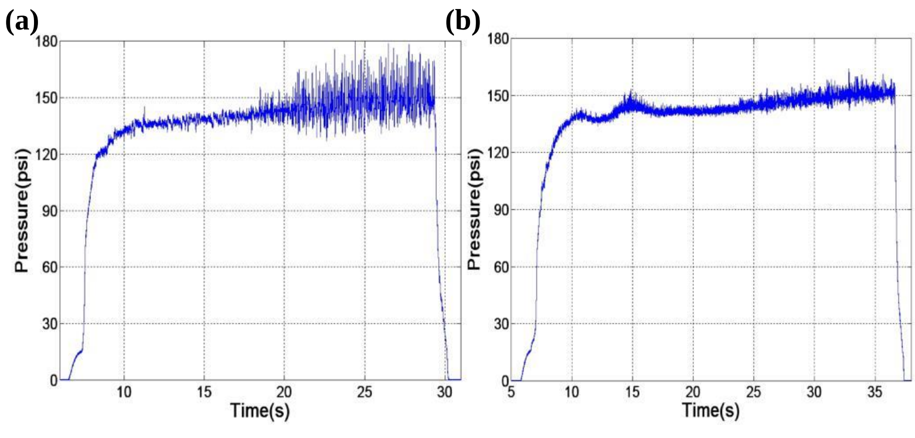

Fig. 3.2.2. Pressure trajectories with a rear diaphragm (a) Test 9(φ=24mm) (b) Test 10(φ =28mm)

Fig. 3.2.2. shows pressure traces in each case tested with a rear diaphragm. The amplification of oscillations occurred at the instant where fuel diameters regressed toward the diaphragm diameter of 24mm. Unlike the pressure curves in Test 3, the LFI sustained to oscillate without any damping until the end of the test. In Test 10 with a rear diaphragm of φ=28mm, the pressure amplification similarly

occurred again even though the amplitudes were smaller than those in Fig. 3.2.2. (a). Based on the results with diaphragms, the initiation of LFI seemed directly related to the time variation of fuel inner diameters or somehow the change in combustion chamber volume due to the fuel regression.
Fig. 3.2.3 displays the frequency peaks of pressure curves in each test case (a) and (b) in Fig. 3.2.3 Peak frequencies in both cases lied in the same frequency range of 11~17Hz as ones previously identified in Test 3.

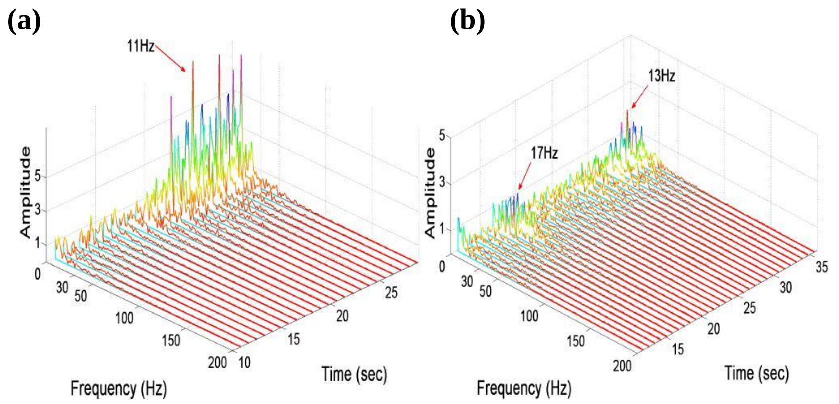

Fig. 3.2.3. Peak frequency in LFI with rear diaphragms (a) Test 9(φ=24mm) (b) Test 10(φ =28mm)

4. Conclusion

A series of experimental tests was designed and performed with selected parameters, including volume ratios between main and post chambers, oxidizer mass flow rates, fuel types and backward facing step configurations in the post chamber. Pressure oscillations in Test 3 suddenly jumped into unstable mode, leading to LFI with a peak frequency of 14~17 Hz. The dominant frequency of 14~17 Hz in Test 3 was interestingly the same frequency as those observed in the stable combustion. Moreover, results in Tests 3, 6-8 and 15 suggested that the occurrence of LFI was insensitive to the change in the material property of solid fuel, and oxidizer mass flows. Interestingly, the initiation of instability was closely associated with the change in flow dynamics induced by the modification of combustion chamber configuration during the combustion. In addition, the results with rear diaphragms confirmed that the time variation of height of backward facing step due to fuel regression significantly affected the instability characteristics by reducing peak amplitudes and changing initiation patterns, but it could not completely alter the occurrence of LFI.

References

1) Jenkins, R.M., Cook, J.R.: *A Preliminary Analysis of Low Frequency Pressure Oscillations in Hybrid Rocket Motors*, 31th Joint Propulsion Conference and Exhibit, AIAA 95-2690, 1995.
2) Lee, C.: *The Application of ZN Analysis to the Transient Combustion of Hybrid Rocket*, 40th AIAA Aerospace Sciences Meeting & Exhibit, AIAA 2002-0783, 2002.
3) Karabeyglu, A., De Zilwa, S., Cantwell, C., and Zilliac, G.: *Modeling of Hybrid Rocket Low Frequency Instabilities*, Journal of Propulsion and Power, Vol.21, 2005, pp.1107~1116.
4) Boardman, T.A., Carpenter, R.L., and Claflin, S.E.: *A Comparative Study of the Effects of Liquid-Versus Gaseous-Oxygen Injection on Combustion Stability in 11-inch-Diameter Hybrid Rocket*, 33th Joint Propulsion Conference and Exhibit, AIAA 97-2936, 1997.
5) Korting, P.A.O.G, Shoyer, H.F.R., and Van der Geld, C.W.M.: *On the use of an Ultrasonic Pulse-Echo Technique for Regression rate Analysis*, SFCC-publication, No. 24, 1987.
6) Carmicino, C.: *Acoustic, Vortex Shedding, and Low-Frequency Dynamics Interaction in an Unstable Hybrid Rocket*, Journal of Propulsion and Power, Vol. 25, No. 6, 2009.
7) Park, K., Shin, K., Lee, C.: *Vortex shedding and Pressure Oscillations in Hybrid Rocket*, KSAS Journal, Vol. 41, No. 1, 2013, pp. 40-47.
8) Wooldridge, C. E., Marxman, G. A., and Kier, R. J.: *Investigation of Combustion Instability in Hybrid Rocket*, NASA CR-66812, 1969.